Influence of the Atchafalaya River on recent evolution of the chenier-plain inner continental shelf, northern Gulf of Mexico

A.E. Draut, G.C. Kineke, D.W. Velasco, M.A. Allison, R.J. Prime

Abstract

This study examines the influence of the Atchafalaya River, a major distributary of the Mississippi River, on stratigraphic evolution of the inner continental shelf in the northern Gulf of Mexico. Sedimentary, geochemical, and shallow acoustic data are used to identify the western limit of the distal Atchafalaya subaqueous delta, and to estimate the proportion of the Atchafalaya River's sediment load that accumulates on the inner shelf seaward of Louisiana's chenier-plain coast. The results demonstrate a link between sedimentary facies distribution on the inner shelf and patterns of shoreline accretion and retreat on the chenier plain. Mudflat progradation on the eastern chenier-plain coast corresponds to the location of deltaic mud accumulation on the inner shelf. On the central chenier-plain shelf, west of the subaqueous delta, relict sediment is exposed that was originally deposited between ~ 1200 and 600 years BP during activity of the Lafourche lobe of the Mississippi Delta complex. Mass-balance calculations indicate that the eastern chenier-plain inner shelf and coastal zone form a sink for 7±2% of the sediment load carried by the Atchafalaya River.

1. Introduction and objectives

Understanding the processes and pathways of sediment dispersal from a fluvial source in a shallow marine environment is a first-order research concern in modern and

ancient sedimentary systems. The goal of this study is to improve constraints on the factors that govern fine-grained sedimentation and geomorphic evolution on the chenier plain of western Louisiana, a classic area for the study of mud-dominated sedimentary systems. To better define nascent stratigraphic development within the young Atchafalaya sedimentary system, this study has examined temporal and spatial evolution of deltaic sedimentary facies on the inner continental shelf. The results link inner-shelf facies distribution to coastal geomorphic variability, and allow estimation of a sediment budget for Atchafalaya River deposits on the shelf.

1.1. The Mississippi–Atchafalaya River system

Quaternary development of the Mississippi Delta complex was affected by continental glaciation and the corresponding decrease in eustatic sea level, which reached a minimum at ~18 kyr (~120 m below present; Fairbanks, 1989). During this sea-level lowstand, Mississippi sediment was delivered to the outer edge of the continental shelf while fluvial channels incised the shelf and older deltaic deposits. After 18 kyr, as Holocene sea level rose, fluvial sediment filled alluvial valleys (~18–9 kyr) and then, after ~9 kyr, began to construct the modern delta plain (e.g., Coleman, 1988; Tye and Coleman, 1989; Saucier, 1994). Since the last glacial maximum, the Mississippi River has built six major delta lobes onto the continental shelf of the northern Gulf of Mexico (Fig. 1, Table 1). Each delta lobe was at one time the primary locus of river deposition (Frazier, 1967; Coleman, 1988). Four of the six lobes are relict features that no longer receive sediment but are subsiding and being reworked by waves. The fifth, the

Balize Delta lobe, has been the active Mississippi depocenter for the past 800–1000 years (Coleman, 1988; Saucier, 1994; Roberts, 1997). The sixth, at the mouth of the Atchafalaya River, represents a new lobe being built at the western edge of the delta complex as the Mississippi has begun to abandon the Balize course in favor of the Atchafalaya route.

Diversion of Mississippi flow to the Atchafalaya had occurred by the 16th century, as a meander bend of the Mississippi intersected the Red River, whose course below the capture site was known as the Atchafalaya. In 1963, the US Army Corps of Engineers completed a control structure that maintains the proportion of Mississippi discharge carried by the Atchafalaya at no more than 30%. As Atchafalaya discharge increased naturally prior to construction of the control structure, the intrabasin lakes and swamps filled with sediment (e.g., Tye and Coleman, 1989). By the 1950s these were largely full, and a subaqueous delta had begun to form in shallow Atchafalaya Bay (Rouse et al., 1978; Van Heerden and Roberts, 1980, 1988; Roberts et al., 1997). Subaerial exposure of the
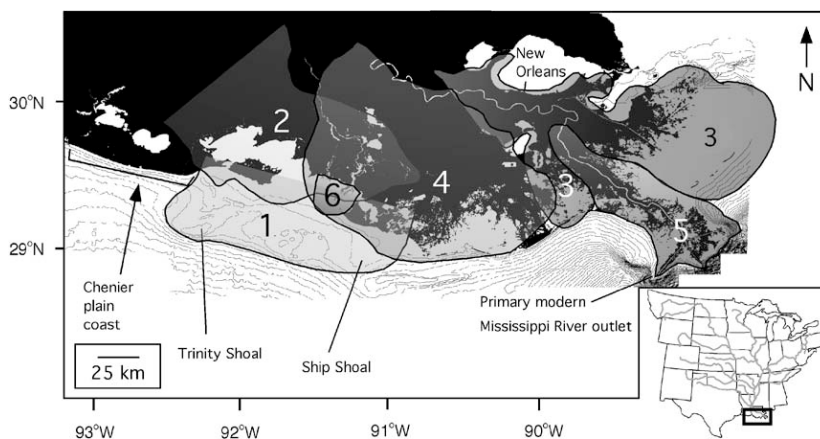
Fig. 1. Six major depocenters of the Mississippi Delta complex that have developed since 9 kyr. In order from oldest to youngest, these are the Maringouin (1), Teche (2), St. Bernard (3), Lafourche (4), modern (Plaquemines–Balize, 5) and Atchafalaya (6) lobes. Figure modified from Penland et al. (1990), based on radiocarbon dating work of Frazier (1967). Within each major lobe there are between three and six smaller sub-lobes (not shown). Bathymetric contour interval is 2 m. Inset map shows drainage basin of the Mississippi River, with box indicating enlarged area of the Mississippi Delta.

Table 1 Age of activity of delta lobes on the Mississippi

Source	Maringouin	Teche	St. Bernard	La
Brannon et al. (1957)	5600–	3800	2750	15
McFarlan (1961)	5600–	3800–2800	2750–2200	15
Saucier (1963)[c]		4600–3600	2800	
Frazier (1967)	7300–6200	5700–3900	4600–700	35
Penland et al. (1987)	7220–3340			24
Coleman (1988)[a]	7500–5000	5500–3800	4000–2000	25
Törnqvist et al. (1996)			3570–	14
Roberts (1997)[a]	7500–5000	5500–3800	4000–2000	25

Delta Plain, in years BP, obtained from eight studies

Note: Papers by Coleman (1988) and Roberts (1997) are review papers. Ages of first activation vary depending upon sampling strategy used in each study. Not all studies obtain an age of latest activity for each lobe. Penland et al. (1987)

have interpreted the Maringouin and Teche lobes as one continuous zone of deposition.

[a]Review paper.

[b]The trunk stream of the Lafourche lobe carried a small flow volume until 1904, when a dam was constructed at its upstream end.

[c]Lobe names used by Saucier (1963) differ from those used by others.

Atchafalaya Delta was first noted after floods in the early 1970s. The Atchafalaya now carries ~84 x 10^6 metric tons of sediment annually (Allison et al., 2000), in comparison to the ~210 x 10^6 metric tons of sediment carried by the combined Mississippi–Red-Atchafalaya system (Milliman and Meade, 1983).

Many studies have examined channel migration and lobe development in the Mississippi Delta. Classic papers include the work of Trowbridge (1930), Fisk (1944), Kolb and Van Lopik (1958), Scruton (1960), Coleman and Gagliano (1964, 1965), and Coleman (1988). Models of delta development based on radiocarbon dates (Fisk and McFarlan, 1955; Brannon et al., 1957; McFarlan, 1961; Saucier, 1963) were modified by Frazier (1967), in a study that has formed the basis for most general interpretations of the Mississippi Delta (Fig. 1). Frazier (1967) showed that a new major depocenter (~30, 000 km^2) has been initiated every 1500–2000 years. Within each of the six major lobes there are 3–6 sub-lobes (e.g., Penland et al., 1987; Roberts, 1997); smaller crevasse splays and overbank deposits form

as natural levees are breached or overtopped. Major distributary channels are now controlled by artificial levees. Recent studies (e.g., Penland et al., 1987; Levin, 1991; Törnqvist et al., 1996) have modified details of depocenter activity determined by Frazier (1967). The chronology of activity within the delta complex varies between studies, which have employed different sampling strategies to quantify the age of first activation in a given channel. Recognition of ancient depocenters, and the times at which they were active, assist interpretation of stratigraphic evolution on the inner shelf.

1.2. The chenier-plain coast and inner continental shelf

The recent development of the Atchafalaya River as a Mississippi River distributary and prominent sediment source has attracted much research attention. This locality offers an opportunity to study a young sedimentary system, and coastal Louisiana has become a classic area in which to investigate fine-grained sedimentary processes (e.g., Wells and Kemp, 1981; Wells and Roberts, 1981; Kemp, 1986; Roberts et al., 1987, 1989; Huh et al., 1991, 2001). The Louisiana chenier plain is the archetypal example of a chenier-plain coast (Russell and Howe, 1935; Byrne et al., 1959; Gould and McFarlan, 1959; Hoyt, 1969; Otvos and Price, 1979; Penland and Suter, 1989). This chenier plain begins 130 km west of the Atchafalaya River outlet and is ~200 km long (Fig. 2). Shore-parallel ''chenier'' ridges 1–3 m high composed of coarse sand and
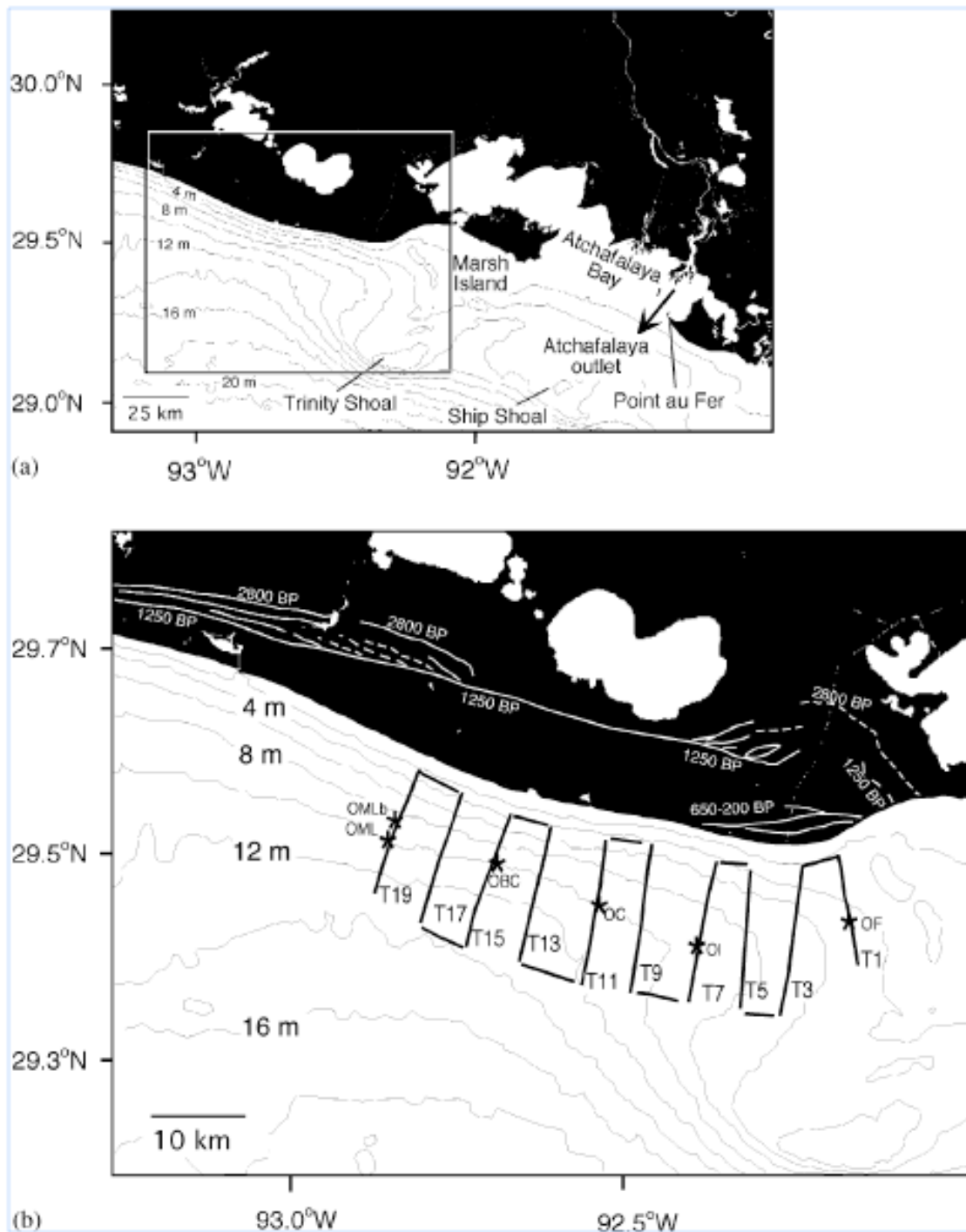
Fig. 2. (a) Atchafalaya River and chenier-plain area,
showing the outlet of the Atchafalaya River entering
shallow Atchafalaya Bay. Relict sediments of the
Maringouin–Teche Delta lobes form Trinity and Ship

Shoals. Contour interval is 2 m. Box indicates area enlarged in Fig. 2b. (b) Detail of the chenier-plain study area, showing (with white lines onshore) chenier ridges with radiocarbon dates obtained by Gould and McFarlan (1959). Dates indicate alternating accretion and erosion on the chenier plain, linked to activity on the Mississippi Delta complex. The ''2800 BP'' line is the oldest shoreline, and represents the extent to which transgression occurred while the St. Bernard lobe was active (Penland and Suter, 1989; see Table 1). Intermediate chenier ridges immediately seaward of the 2800-BP shoreline represent activity of different sub-lobes within the Lafourche lobe. The coast seaward of the 1250-BP shoreline accreted during activity of the Lafourche lobe, between 1250 and 600 BP. When the Lafourche lobe was abandoned in favor of the Mississippi's modern course, accretion on the chenier plain ceased and the youngest chenier ridges formed (650–200 BP shoreline). Modern accretion due to Atchafalaya sediment delivery occurs seaward of these youngest chenier ridges. Locations of sediment cores (OF, OI, OC, OBC, OMLb) are shown on the inner shelf, as are acoustic transects T1–T19. At Site OML, core collection was unsuccessful due to a resistant sea floor.

shells alternate with marshes that represent relict mudflat zones (Gould and McFarlan, 1959; Byrne et al., 1959; Beall, 1968; Hoyt, 1969; Otvos and Price, 1979). This shoreline began to develop ~3000 years ago (Gould and McFarlan, 1959)as mudflats prograded when the Mississippi River delivered sediment to the western edge of its delta complex. When fluvial deposition shifted farther

east, reducing sediment supply to the chenier plain, mud deposits were reworked and the coarse lag sediment rich in shell debris was concentrated into the ridges (i.e., cheniers) that separate marsh zones (Gould and McFarlan, 1959; Penland and Suter, 1989; Augustinius, 1989).

Rapid coastal retreat occurs on most of Louisiana's shoreline (e.g., Gagliano et al., 1981; Penland and Ramsey, 1990; Penland et al., 1990, 2000; Westphal et al., 1991; Williams, 1994) due to subsidence and compaction of the delta plain, eustatic sea-level rise, and human activity that reduces sediment delivery to the delta. Mudflat accretion on the eastern chenier-plain coast is therefore atypical for the northern Gulf of Mexico shoreline. Prior studies of the chenier-plain area have focused on coastal geomorphic evolution, and in particular on mudflat progradation in response to sediment delivery from the Atchafalaya River (Morgan et al., 1953; Gould and McFarlan, 1959; Byrne et al., 1959; Beall, 1968; Wells and Roberts, 1981; Wells and Kemp, 1981; Kemp, 1986; Roberts et al., 1987, 1989, 2002; Huh et al., 1991, 2001; Draut, 2003). Mudflat accretion on the eastern chenier plain occurs in response to shoreward sediment transport and onshore deposition during the passage of winter cold fronts and occasional large storms, implicating energetic events as important mechanisms by which inner-shelf sediment is resuspended and transferred to coastal mudflats (Morgan et al., 1958; Kemp, 1986; Roberts et al., 1987, 1989; Penland et al., 1989; Huh et al., 1991, 2001; Kineke, 2001a, b; Draut, 2003; Rotondo and Bentley, 2003).

1.3. Previous investigations on the western Louisiana shelf

A majority of sedimentary studies of the northern Gulf of Mexico coast have concentrated on the Mississippi Delta plain, including the studies of delta lobe development and chronology discussed above. Thompson (1951) first described subaqueous Atchafalaya sediment deposits within Atchafalaya Bay and seaward of the Point au Fer shell reef (Fig. 2a). Schlemon (1975) and Rouse et al. (1978) first investigated the subaerial delta in Atchafalaya Bay. Sedimentary studies of the subaerial and shallow subaqueous Atchafalaya Delta by Roberts et al. (1980), and by Van Heerden and Roberts (1980, 1988), allowed reconstruction of annual-scale development within this system.

Allison et al. (2000) used ^{210}Pb, ^{137}Cs, and ^{7}Be geochronology from sediment cores to constrain seasonal and decadal-scale accumulation rates at four stations on the shelf west of the Atchafalaya outlet, and evaluated reworking of sediment due to winter cold front passage. Gordon et al. (2001) used organic geochemical data to constrain patterns of organic carbon and total nitrogen accumulation on the subaqueous Atchafalaya Delta, and inferred a partial sediment budget for this system (see Section 4.1.3). Allison and Neill (2002) and Neill and Allison (submitted) analyzed sedimentary facies and accumulation rates on the distal subaqueous delta, combining core data with Chirp reflection profiles in a study that forms a basis for comparison with this work. The inner-shelf seaward of the chenier plain lies between the subaqueous Atchafalaya Delta and, to its west, an area characterized by minor amounts of sediment delivered by

the Brazos and Trinity Rivers in eastern Texas and the Atchafalaya coastal current. Morton and Winker (1979) assessed the distribution of coarse clastic and biogenic sediments on the Texas shelf west of the chenier plain. Morton (1981) correlated stratigraphic horizons representative of storm events to measured storm-induced bottom currents on the Texas inner shelf. This study builds upon previous investigations of fine-sediment dispersal near shore by examining stratigraphic development on the western subaqueous Atchafalaya Delta and by placing regional mass-balance constraints on Atchafalaya sedimentation.

2. Methods

Shallow acoustic data and core stratigraphy are used to assess facies variation and stratal geometry. Data were collected using the *R/V Eugenie* in 2001. Fig. 2b shows the locations of acoustic transects and core sites used to ground-truth the shallow seismic record.

2.1. Core collection and sediment sampling

Five cores were collected at regularly spaced intervals on shore-perpendicular acoustic transects using a kasten corer (Fig. 2b; Kuehl et al., 1985; Zangger and McCave, 1990). The core was X-rayed with a Kramex model PX-20N machine at 15 mA/70 keV in 0.3-m segments. Sediment was sampled at 0.05-m intervals, with each sample containing 0.02 m of vertical thickness. Additional samples were collected at depths where facies changes were observed.

2.2. Grain-size and porosity analyses

Porosity calculations were made using 13–20 g of wet sediment. Samples were dried in an oven at 50–60°C and the dry weight was used to calculate porosity and bulk density (Lee and Chough, 1987), using a sediment density of 2650 kg/m^3 and a seawater density of 1010 kg/m^3. Grain-size analyses used 2–8 g (dry mass) of sediment per sample. Sediment was disaggregated and homogenized using an ultrasonic probe and a mechanical stirring device to agitate a slurry of sediment in 0.1% sodium metaphosphate solution used as a dispersant. The sand fraction was separated using a 63 μm (4.0ϕ) sieve, dried, and weighed. The silt–clay fraction (< 63 μm) was analyzed using a Micromeritics SediGraph 5100 particle size analyzer at Boston College (McCave and Syvitski, 1991; Coakley and Syvitski, 1991; Micromeritics, 2001). Details of sample preparation and instrument operation can be found in Draut (2003). The sand fraction (> 63 μm) of each sample was sieved at even ϕ intervals to determine the grain-size distribution within this coarse fraction. Observations of sediment composition were made using a binocular microscope.

2.3. Isotope-activity measurement

Inventories of ^{210}Pb and ^{137}Cs were measured on selected sediment samples. These isotopes have been used in near-shore sedimentation studies to assess accumulation rates (e.g., Nittrouer et al., 1979; Smith and Walton, 1980; Allison et al., 1995a, b, 1998, 2000; Jaeger and Nittrouer, 1995; Kuehl et al., 1995; Goodbred and Kuehl, 1998). The isotope ^{210}Pb, a naturally occurring daughter product of ^{238}U, has a half-life of 22.3 years. Measurement of excess-

^{210}Pb inventory (that which exceeds the ^{210}Pb activity supplied to sediment by in situ decay of its grandparent 226

Ra via ^{222}Rn) allows estimation of accumulation rates in sediment deposited within the past 100 years. In contrast, ^{137}Cs is an isotope with a 30-year half-life produced by hydrogen bomb testing; its presence indicates that sediment has been in contact with an atmospheric or fluvial source more recently than ~1950, when ^{137}Cs was introduced to the environment (e.g., Livingston and Bowen, 1979; Miller and Heit, 1986).

Activities of ^{137}Cs and excess ^{210}Pb were determined by gamma counting (Gäggler et al., 1976) on selected samples from Cores OF, OI, OBC, and OMLb (Fig. 2b). Frozen sediment samples were freeze-dried and disaggregated in a desiccation chamber at the US Geological Survey laboratory in Woods Hole, MA, and homogenized prior to gamma counting; 8–10 g (dry mass) of sediment was analyzed per sample. Samples were analyzed on Canberra model GCW 3023 pure germanium well detectors at the University of Rhode Island for 48–96 h (e.g., ^{210}Pb error < ± 3%). Efficiency corrections were empirically determined using an Analytics Co. mixed gamma standard for detector calibration (SRS#51276–399). Activities of ^{137}Cs and Pb were measured using net counts of the 661.6 and 46.5 keV peaks, respectively; excess-^{210}Pb activity was calculated from independent measurement of ^{214}Pb at 352 keV (Joshi, 1987).

Three samples of carbonate shell material were selected for ^{14}C age analysis: one from the base of Core OF at a depth of 1.56 m below the sea floor (bsf), one from a prominent horizon of large shells in Core OBC (0.51 m bsf), and one from Core OMLb (0.41 m bsf). Samples were prepared and analyzed by accelerator mass spectrometry at Geochron Laboratories in Cambridge, MA. The analytical error is ± 1% based on analysis of a laboratory standard with 95% of the activity of an NBS oxalic acid standard. Ages are based upon the ^{14}C half-life of 5570 years and are reported in years referenced to the year 1950. To adjust these ages into time before 2003, 53 years have been added. A reservoir correction (Stuiver et al., 1986) of 200–400 years was made, based on rapid transition from terrestrial to marine organic carbon compounds in surface sediment away from the Mississippi and Atchafalaya Rivers (Goñi et al., 1998).

2.4. Shallow acoustic surveys

Shallow stratigraphy was investigated using a Knudsen echo sounding system mounted on the *R/V Eugenie*. The Knudsen 320B/P dual-fre-quency echo sounder emits an acoustic signal at 50 and 200 kHz simultaneously, with beam widths of 6–10° and 17–31°, respectively (Knudsen Engineering, 1996). The instrument converts re-turn-time data to depth using an acoustic velocity of 1500 m/s. The signal is processed through a band-pass filter with its pass band centered at the transmitted frequency. The echo sounder yields depth to sea bed and shallow stratigraphy within ~5 m through relatively unconsolidated fine sedi-ment (Velasco, 2003). A Northstar[TM] differential GPS unit was interfaced with the echosounder during operation.

Acoustic data were obtained along 19 transects that covered a total area of approximately 680 km^2 (Fig. 2b).

3. Results

3.1. Sedimentary facies

Results of facies analyses are shown in Fig. 3. Stratigraphic depths have been adjusted to account for angle of penetration of the core barrel into the sea floor, determined from X-radiographs. Cores OF and OI (Figs. 3a and b), collected seaward of the eastern chenier-plain coast, were dominated by a poorly consolidated mud layer. This heavily bioturbated unit showed homogeneous porosity (average 74%) and grain-size distribution, with dark mud oxidizing to a brown color after several minutes of exposure to air. Clay and silt comprised ~74% and 25% by mass, respectively, with trace amounts of siliciclastic and carbonate sand. At the base of the poorly consolidated mud layer in Cores OF and OI, an abrupt transition occurred to sandier, more consolidated sediment. At both sites the core barrel was rejected at this coarse layer, which contained > 15% sand by mass with 70% porosity. The upper part of Core OC (Fig. 3c) contained a mud unit similar to that which dominated Cores OF and OI, with 0.74 m of poorly consolidated, bioturbated dark mud (average porosity 73%; 87% clay and 12% silt by mass with trace siliciclastic and carbonate sand). At 0.74 m bsf, the mud was underlain by several sandy horizons. Porosity was 54–55% in the basal sand/shell material, which contained 60% sand by mass (nearly all siliciclastic grains).

Cores OBC and OMLb, collected on the central chenier-plain shelf, lacked the homogeneous soft mud that dominated Cores OF, OI, and upper OC, and showed lower porosity than the eastern cores. The uppermost section of Core OBC contained consolidated sediment with sand and shell fragments (> 50% sand-sized grains by mass at the core top). Several sandy mud horizons occurred in Core OBC (Fig. 3d). Sand content decreased to 12% at the base of the core (0.8 m bsf), corresponding to an increase in the proportion of clay.

At Site OML, the 310-kg kasten core barrel was unable to penetrate consolidated sediment at the sea floor (Fig. 2b). As a substitute for this planned core site, Core OMLb (Fig. 3e) was obtained where the sea floor was soft enough to permit core recovery. The uppermost 0.08 m of this core consisted of stiff mud with shell fragments (porosity 67%). From 0.08 to 0.46 m bsf, the core contained consolidated mud (average porosity 67%, 84.4% clay with 12.5% silt and minor carbonate sand). This horizon contained millimeter-scale planar bedding. At 0.41 m bsf, a 0.01-m-thick sand and shell horizon occurred. Below that, the core contained stiff mud with the consistency of modeling clay (average porosity 63% but locally as low as 52%; average

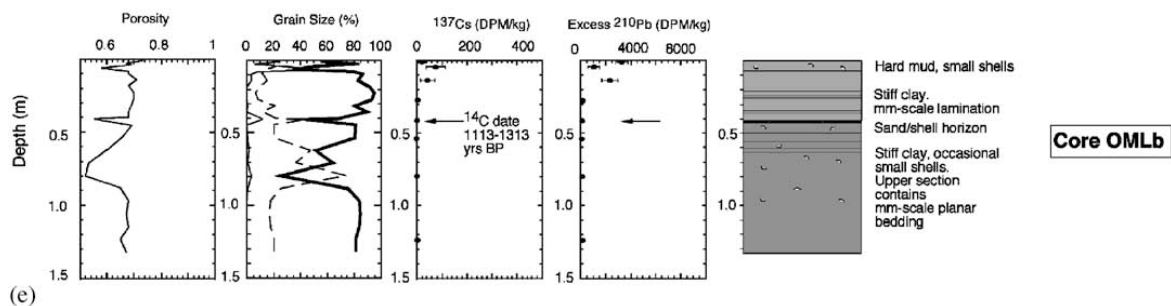64% clay, 34% silt, with minor carbonate sand).

(a) Core OF

(b) Core OI

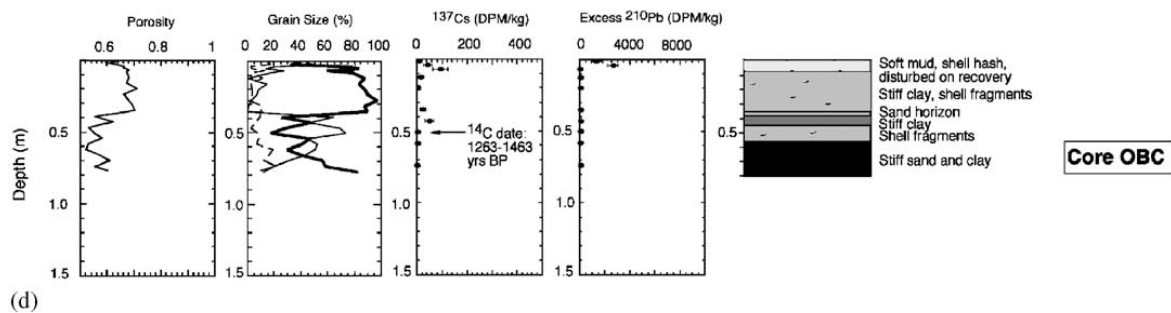(c) Core OC
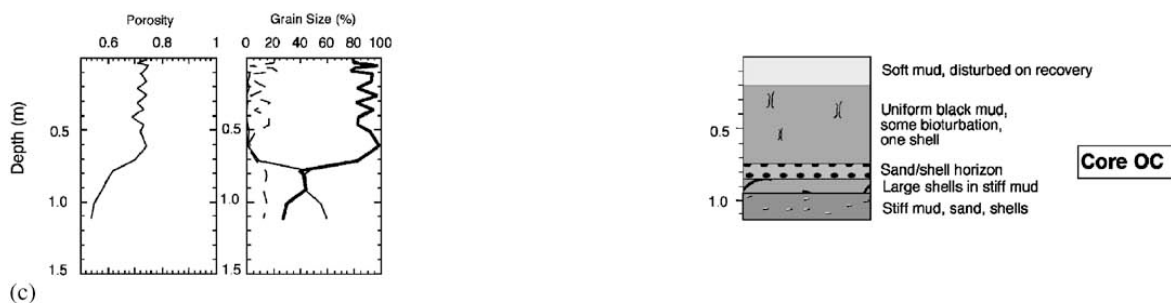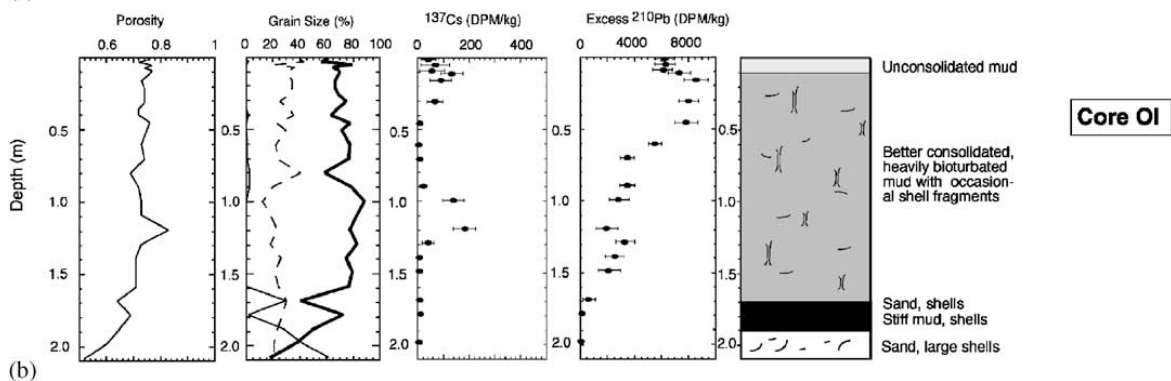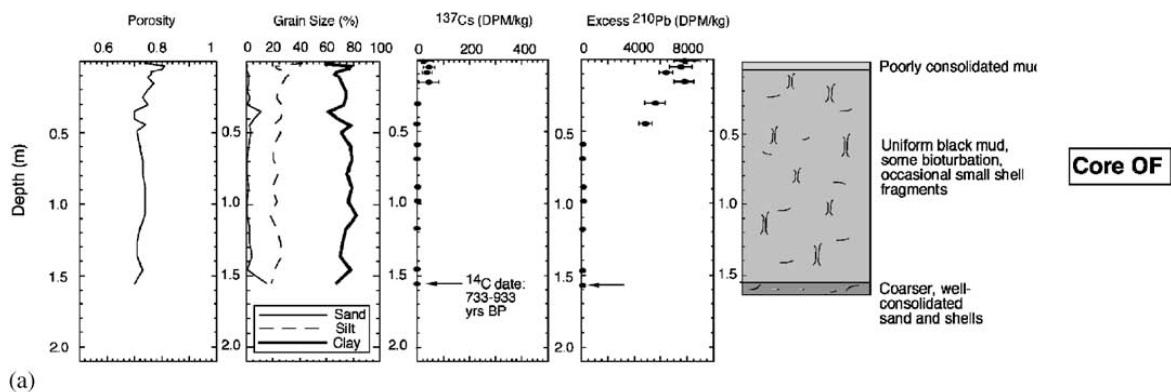
(d) Core OBC

(e) Core OMLb

Fig. 3. Sedimentary facies data and isotope stratigraphy from sediment cores. Stratigraphic diagrams were compiled from field observations during core sampling and are presented alongside grain size, porosity, and, if available, ^{137}Cs and excess-^{210}Pb data. The easternmost core (Core OF) is at top, followed in order by cores collected increasingly farther west: Cores OI, OC, OBC, and OMLb. Individual sediment samples are 0.02 m thick.

Table 2
Results of radiocarbon dating of shell material from one shell horizon each in Cores OF, OBC, and OMLb

Core	Sample depth (m bsf)	Reported age	Age in years BP	Reservoir-corrected age
OF	1.56	1080±50	1133±50	733–933±50
OBC	0.51	1610±60	1663±60	1263–1463±60
OMLb	0.41	1460±30	1513±30	1113–1313±30

Note: The sample depth listed is the center of a 2-cm thick sample. The reported age is that found directly from ^{14}C analysis (referenced to the year 1950). Fifty-three years have been added to the reported age to obtain age in years BP. An additional reservoir correction has been made to account for incorporation of isotopically old carbon in modern shells. The reservoir adjustment of 200–400 years is made in accordance with the method of Goñi et al. (1998), based on Stuiver et al. (1986).

3.2. Isotope stratigraphy

The supported ^{210}Pb activity was determined from isotopic profiles in Cores OF and OI to be ~1000 DPM/kg, a value consistent with that obtained by direct measurement of

[214]Pb activity. This supported ^{210}Pb activity is similar to that observed in relict fine-grained sediment on the Texas inner shelf (Holmes, 1985). Cores OF and OI (Figs. 3a and b) contained excess ^{210}Pb in the uppermost sediment of each core. At Site OF, ^{210}Pb defined a surface mixed layer (SML) of ~0.17 m, and reached the supported activity at ~0.55 m bsf. No apparent sedimentary facies transition accompanied the isotopic transition to supported activity. The upper 0.15 m of this core contained ^{137}Cs, but at activities near the lower detection limit. At Site OI, the pattern of decreasing excess-^{210}Pb activity was irregular. The SML was between 0.1 and 0.4 m thick; supported activities occurred below a thin sand horizon at ~1.60 m bsf. The upper 0.30 m of Core [137]OI contained [137]Cs. A second peak in Cs activity occurred from 0.95 to 1.30 m bsf in Core OI (Fig. 3b). Isotope analyses were not made on Core OC. Cores OBC and OMLb showed low activities of excess ^{210}Pb and ^{137}Cs throughout the core, with a thin or absent SML. Excess ^{210}Pb and ^{137}Cs were present in the upper 0.07 m of Core OBC. Core OMLb (Fig. 3e) contained both isotopes in its uppermost ~0.12 m; below that, ^{137}Cs was not detected, and ^{210}Pb was present only at background activities.

Radiocarbon ages of shell material obtained from Cores OF, OBC, and OMLb are presented in Table 2. The basal shell horizon in Core OF (from a depth of 1.56 m bsf) yielded an age of 733–933±50 years BP, after reservoir correction (Goñi et al., 1998). A shell layer in Core OBC that spans 0.49–0.51 bsf yielded an age of 1263–1463±60

years BP after reservoir adjustment, and a shell horizon in Core OMLb (0.41 m depth bsf) yielded an adjusted age of 1113–1313±30 years BP.

3.3. Shallow acoustic transects

The easternmost shore-perpendicular acoustic transect, T1, revealed bedding that dipped gently seaward (Fig. 4a), with a reflector at 1.7 m bsf that coincides with the depth of the basal sand/ shell layer in Core OF. The shoreward portion of Transect T1 shows a disturbed sea bed, possibly due to trawling by fishing vessels. Profile T3, ~10 km west of T1, shows sigmoidal clinoforms (defining a stratigraphic unit up to 5 m thick; Fig. 4b). In Transects T5 (not shown) and T7 (Fig. 4c), some bedding parallel to the sea floor is apparent but evidence of significant accretion and foreset development are absent; the sea floor geometry is convex landward of 8 m water depth. Core OI, collected ~13.5 km offshore along Transect T7,
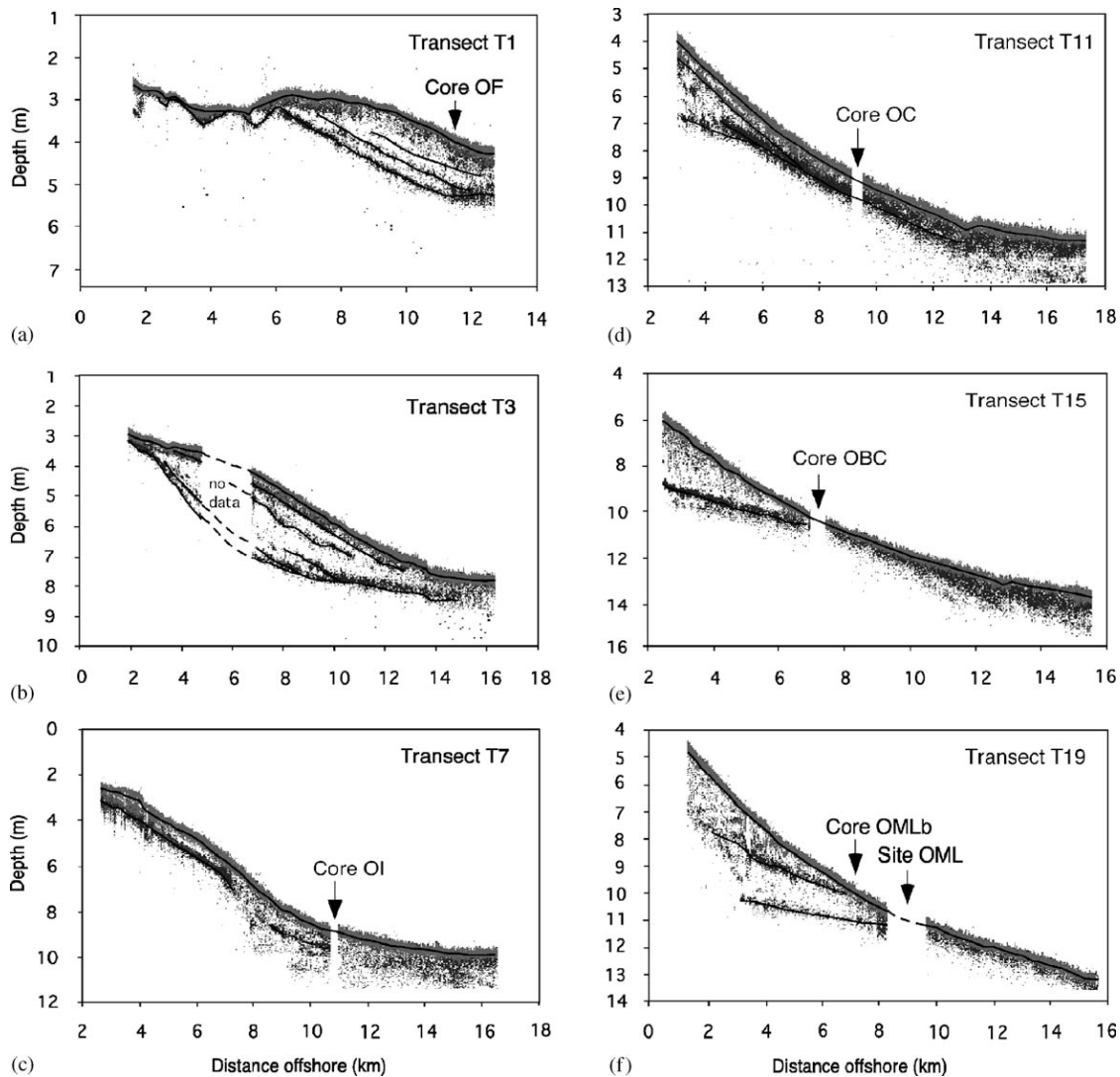
Fig. 4. Selected shore-perpendicular acoustic transects from the eastern and central chenier-plain shelf (locations in Fig. 2b). Transect T1 (a), the easternmost profile, is disturbed at its landward end, possibly due to trawling activity by fishing boats; the seaward part of T1 indicates beds that dip gently seaward. Transect T3 (b) shows a convex sea floor that defines the upper surface of a sigmoidal clinoform. Transects T7 (c) and T11 (d) indicate a gradual westward transition from convex to concave sea floor. Transects T15 (e), T17 (not shown), and T19 (f) show acoustic reflectors

truncated by a sea floor that dips seaward more steeply than the bedding angle; this geometry suggests relict sigmoidal clinoforms that have undergone erosion.

contained basal shell horizon at 1.88 bsf that approximately coincides with the deepest reflector in Transect T7 beneath Site OI.

Transect T11 contains sub-sea-floor reflector that pinches out in the seaward direction (Fig. 4d). Core OC was collected ~9.5 km offshore along T11. Beneath that site, reflector coincides approximately with the depth in Core OC at which transition occurred between soft mud and coarser facies with lower porosity(0.74 bsf). The sea-floor geometry in Transects T11–T19 is broadly concave, in contrast to the sigmoidal profiles east.

All transects west of T11 display one or two reflectors that are truncated by intersection with the sea floor; the sea floor dips seaward more steeply than the bedding. Transect T15 (Fig. 4e) shows one dominant reflector ~0.3–0.4 m bsf at Site OBC, approximately the depth at which sediment in Core OBC undergoes a downward transition from mud to lower porosity, coarser facies. At 0.5 m bsf in Core OBC (~0.1 m below the deepest reflector of T15), shell material yielded a radiocarbon age of 1263–1463±60 years BP (Table 2). The westernmost transect, T19, contains two reflectors truncated by the sea floor (Fig. 4f). Core OMLb was collected 6.5 km offshore along T19. A reflector at 0.4–0.5 m bsf at Site OMLb approximately coincided with the depth of a shell horizon (0.41 m bsf) that yielded a radiocarbon age of 1113–1313±30 years BP.

4. Discussion

4.1. Modern sediment accumulation on the chenierplain inner shelf

Sedimentary facies, radioisotope activity, and stratal geometry inferred from shallow acoustic data constrain the degree to which the Atchafalaya River affects sedimentation on the inner-shelf seaward of the chenier plain. These data can be used to calculate decadal-scale accumulation rates, identify the western extent of Atchafalaya sediment accumulation, and define the regional significance of active deposition on the inner-shelf seaward of the chenier plain.

4.1.1. Decadal-scale accumulation: eastern chenierplain inner shelf

Decadal-scale accumulation rates can be calculated from excess-^{210}Pb profiles. Estimation of such long-term accumulation rates reduces the effects of seasonal and annual variability in sediment delivery, which can affect the thickness of the SML. Accumulation rates were obtained using a constant rate of supply (CRS) model (Crozaz et al., 1964; Appleby and Oldfield, 1978). The CRS model assumes that ^{210}Pb is supplied to sediment at a constant rate before its deposition, but that the initial ^{210}Pb concentration in the sediment, and the supply rate of sediment, may vary. This model allows determination of the age of sediment at any given depth in the core, using integrated ^{210}Pb activity below the depth considered. Integrated ^{210}Pb activity was calculated for sediment profiles at Sites OF and OI using interpolation at 0.05-m

intervals between measured values. The sedimentation rate is

$$S = \frac{-\lambda z}{\ln(A_z/A_0)}, \quad (1)$$

where A_0 is the total excess-^{210}Pb activity in the core and A_z is the excess-^{210}Pb activity below depth z. Accumulation rates were calculated using sediment depths that had been adjusted to 75% porosity to eliminate the effects of compaction on accumulation rate.

Using this CRS model, the century-averaged accumulation rate for Core OF is 0.94 cm/yr (9.4×10^{-3} m/yr), with a standard deviation of 0.15 cm/yr (1.5×10^{-3} m/yr). In Core OF, ^{137}Cs inventory is too low to be used for independent verification of the ^{210}Pb-derived accumulation rates. Low activities of ^{137}Cs in sediment from Core OF that contains high excess ^{210}Pb suggests that sediment has been resuspended after its initial deposition. Resuspended sediment could thus have scavenged ^{210}Pb from the water column and possibly mixed with older inner-shelf sediment before being redeposited at this site. Repeated exposure of sediment to new excess ^{210}Pb by resuspension will increase its excess-^{210}Pb inventory while not increasing ^{137}Cs (e.g., Duursma and Gross, 1971; Scrudato and Estes, 1976; Smith and Ellis, 1982; Baskaran and Santschi, 2002). Any

137

Cs in sediment will gradually decay, and may also be remobilized in anoxic pore water (Sholkovitz et al., 1983; Sholkovitz and Mann, 1984). Older sediment advected to Site OF would contain excess ^{210}Pb but little or no ^{137}Cs, and its mixing with more recent fluvial sediment would dilute the ^{137}Cs isotopic signal of recent fluvial input (e.g., Holmes, 1985). Resuspension events on this inner shelf include winter cold fronts, hurricanes, and tropical storms, as well as trawling activity by shrimping vessels. The portion of core sediment that contains no excess ^{210}Pb (the lower sections of Cores OF and OI, as well as the majority of the core thickness at Sites OBC and OMLb) is interpreted to have undergone no resuspension in the past 100 years; any excess ^{210}Pb present at the time of its initial deposition has been lost through isotopic decay.

Profiles of ^{210}Pb and ^{137}Cs in Core OI (Fig. 3b) differed from those of Core OF (Fig. 3a). There is no clear transition in the Site OI ^{210}Pb profile from an upper SML to a region of radioactive decay to a region of supported ^{210}Pb activity. The CRS model yields a century-averaged rate of 2.0 cm/yr (2.0 x 10^{-2} m/yr) and a standard deviation of 0.29 cm/yr (2.9 x 10^{-3} m/yr). With an accumulation rate of ~2 cm/yr (0.02 m/yr), the lower limit of ^{137}Cs (representing the year 1950) would be expected to occur at 1.00 m bsf. A peak in ^{137}Cs occurs slightly below that depth, reaching ~180 DPM/kg in a broad peak that spans >0.30 m of sediment (Fig. 3b). Above this peak,

137

Cs is absent between 0.40 and 0.90 m bsf, and occurs in the SML at an activity slightly lower than in the deeper peak. It is possible that this

^{137}Cs profile may have resulted from an event that disturbed sediment at this site (e.g., trawling by fishing boats, or oil pipeline installation in the vicinity). Alternatively, a combination of fluvial discharge, resuspension events, and mixing with older inner-shelf sediment could have produced these isotopic profiles, though this cannot be positively ascertained from the core stratigraphy.

The bioturbated nature of sediment in Cores OF and OI in the presence of relatively high accumulation rates suggests that rapid deposition of sediment may occur episodically (as would occur following storms or cold fronts), separated by intervals of slower accumulation and biogenic reworking. Cores with comparable accumulation rates collected nearer to the river mouth, where sediment delivery is largely controlled by continuous fluvial input, are commonly well stratified and without significant bioturbation (Allison and Neill, 2002).

Cores OBC and OMLb, sites seaward of the central chenier plain at which no SML could be clearly identified, contain little to no ^{137}Cs and have ^{210}Pb profiles that reach supported activity almost immediately below the sea floor. The lack

of ^{137}Cs and excess ^{210}Pb in these two cores implies that they contain relict sediment that has not been exposed to the water column within the past 100 years (five half-lives of ^{210}Pb, the detection limit; e.g., Holmes, 1985). Due to the

low isotopic inventory, accumulation rates cannot be calculated for Cores OBC and OMLb. These sites likely receive some sediment seasonally (e.g., Allison et al., 2000), but are not sites of long-term accumulation.

4.1.2. Western extent of Atchafalaya sediment accumulation

Sedimentary facies, isotopic characteristics, and stratal geometry define the western limit of the subaqueous Atchafalaya Delta. In contrast to the coarser particles that are concentrated in a relatively small (tens of km^2) delta lobe at the river mouth, silt and clay form a broad fan of distal sediment that is deposited along and across the shelf, affected secondarily by resuspension events (e.g., Kolb and Van Lopik, 1958; Coleman and Gagliano, 1964; Coleman, 1981; Nemec, 1995; Allison and Neill, 2002). Although aggregation and settling substantially reduce the suspended-sediment concentration in the river plume within 10 km of the river mouth, distal mud of the Atchafalaya Delta covers more than 1000 km^2 (e.g., Coleman, 1981; Van Heerden and Roberts, 1988). Allison and Neill (2002) showed that the proximal subaqueous delta has a maximum thickness of 2.5 m immediately seaward of Point au Fer (at the mouth of the dredged river outlet; Fig. 2a), where accumulation rates exceed 10 cm/yr. Deltaic sediment pinches out seaward of the 8 m isobath as accumulation rates decrease. Atchafalaya sediment grades seaward from proximal, interbedded sandy silt near Point au Fer to more distal clayey silt in water depths from 3 to 7 m (Allison and Neill, 2002). The most distal deposits, where accumulation rates were < 1 cm/yr, contained silty clay affected by bioturbation that had destroyed primary bedding fabric. The

Allison and Neill (2002) study thus constrained the seaward (southern) extent of the Atchafalaya Delta, identified evidence of active progradation in the stratal geometry on the inner shelf, and estimated accumulation rates across much of the subaqueous delta area. This work complements the Allison and Neill (2002) study by identifying the western extent of the distal Atchafalaya Delta and thus further constrains the extent of fluvial-dominated sedimentation on the inner shelf.

The homogeneous, poorly consolidated mud that dominates sediment in the eastern cores of this study (Cores OF, OI, and upper OC) is inferred to be recently derived from the Atchafalaya River. We interpret this layer as distal sediment of the Atchafalaya Delta. This interpretation is consistent with other recent studies (e.g., Rotondo and Bentley, 2002, 2003; Roberts et al., 2002; Velasco, 2003) that have indicated active accumulation of Atchafalaya sediment immediately offshore of the eastern chenier plain. The presence of ^{137}Cs in the uppermost sediment of Cores OF and OI implies a recent source for the sediment, though the elevated excess-^{210}Pb activities compared to those of ^{137}Cs in these cores suggest that scavenging of Pb from seawater and/ or mixing with sediment advected toward shore may have affected this material either during transport to the core sites or during subsequent resuspension events (Section 4.1.1). This distal-deltaic sediment thins westward away from the mouth of Atchafalaya Bay, from >1.5 m thick in Cores OF and OI to 0.74 m thick in Core OC. The dominant particle size of sediment in this layer is similar at Sites OF and OI

(containing an average of 73% clay at Site OF and 75% clay at Site OI), but is finer at Site OC, where the average clay content of the Atchafalaya sediment is 87%. Visual descriptions and X-radiograph images of this sediment were similar to descriptions of Allison and Neill (2002), which found the distal southern delta to be heavily bioturbated and homogeneous with respect to particle size. ^{210}Pb accumulation rates in Cores OF and OI (1–2 cm/ yr) are slightly higher than accumulation rates at the southern edge of the subaqueous delta (0.2–0.5 cm/yr; Allison and Neill, 2002). The basal sand–shell layer that underlies Atchafalaya sediment at Sites OF, OI, and OC compares favorably with the resistant shell-hash facies at the base of Atchafalaya Delta sediment south of the river mouth (Allison and Neill, 2002). Thompson (1951) documented the presence of similar shell hash underlying unconsolidated modern Atchafalaya sediment seaward of Point au Fer.

The stratal geometry within the eastern chenierplain inner shelf supports the interpretation of active sedimentation. Transect T1 shows bedding that dips gently seaward, in the vicinity of Site OF (Fig. 4a). The lowermost acoustic reflector in Transect T1 coincides with the base of deltaic mud in Core OF (1.55 m bsf). It is noteworthy that although Transect T1 crosses relict sediments of the Maringouin and Teche Delta lobes on Trinity Shoal (Fig. 2a), the radiocarbon age obtained for shell material in the basal horizon of Core OF (1.56 m bsf) yielded an age of 730–930 years BP, too young to represent the active phase of those delta lobes

(~3000–7500; Table 1). Transect T3 shows sigmoidal clinoforms dipping seaward that form a discrete sedimentary package 5 m thick (Fig. 4b). The change in stratigraphic configuration between Transects T1 and T3 suggests the presence of topset/foreset beds in T1 and prograding foreset beds in T3. The convex shape of these two cross-shore profiles is consistent with active progradation. Convex inner shelf profiles are common where river sources contain abundant suspended sediment, which causes the distal-delta slope to prograde seaward more rapidly than the delta front (Coleman, 1981; Postma, 1990, 1995).

The geometry in these eastern transects is similar to that of other fine-grained fluvial dispersal systems; sigmoidal clinoforms with distinct topset, foreset, and bottomset beds have been described in mud-dominated subaqueous deltaic deposits of the Amazon (Nittrouer et al., 1986, 1995), Ganges–Brahmaputra (Kuehl et al., 1990), Fly (Harris et al., 1993), and relict Huanghe (Alexander et al., 1991) River systems. The well-developed discrete clinoform package imaged by Transects T1 and T3 suggests that the deposition of Atchafalaya sediment on the eastern chenier-plain shelf comprises a smaller, secondary depocenter of the Atchafalaya system rather than merely representing bottomset beds of the main subaqueous delta. This inference of a secondary depocenter discrete from the primary delta is analogous to the deposition of Huanghe River sediment in a secondary locus (Shangdong peninsula region) in addition to its primary delta (Alexander et al., 1991).

West of Transect T3, distinct clinoform geometry (foreset bedding) was not observed. Stratigraphic geometry in Transects T5, T7, and T9 showed sub-bottom reflectors approximately parallel to the sea floor that may represent along-shelf growth of bottomset beds; the finer grain size and diminished vertical thickness of inferred Atchafalaya sediment at Site OC are consistent with bottomset beds extending as far west as Transect T11. A transition from Atchafalaya Delta mud to relict facies occurs between Sites OC and OBC, coincident with the absence of an overlying accretion layer in the acoustic profiles. This transition, at longitude ~92.55°W, is inferred to mark the western extent of Atchafalaya-dominated sedimentation on the inner shelf. Notably, this longitude approximately coincides with the boundary between coastal areas that experience decadal-scale accretion (eastern chenier plain) and those that currently experience decadal-scale shoreline retreat (based on analysis of historical aerial photographs; Draut, 2003; Draut et al., submitted), illustrated in Fig. 5. Other studies have shown that mudflat accretion on the eastern chenier plain occurs in the presence of an unconsolidated, mud-rich sea bed, from which sediment is resuspended during cold fronts and storm events and provides sediment that accumulates as coastal mudflats (e.g., Huh et al., 1991; Kineke, 2001a, b; Kineke et al., 2001). Stratigraphic relationships on the inner shelf therefore indicate that the extent of the subaqueous Atchafalaya Delta influences the location where coastal mudflat accretion occurs by these processes, because deposition of fluvial silt and clay maintains the

underconsolidated muddy substrate necessary to fuel mudflat growth (Fig. 5).

4.1.3. Significance of the chenier-plain inner shelf in the Atchafalaya River sedimentary system

To assess the proportion of the Atchafalaya River's sediment load that accumulates on the inner-shelf area investigated, the total mass of deltaic sediment represented by these study sites has been estimated. Facies distribution is known to be spatially and temporally variable over this
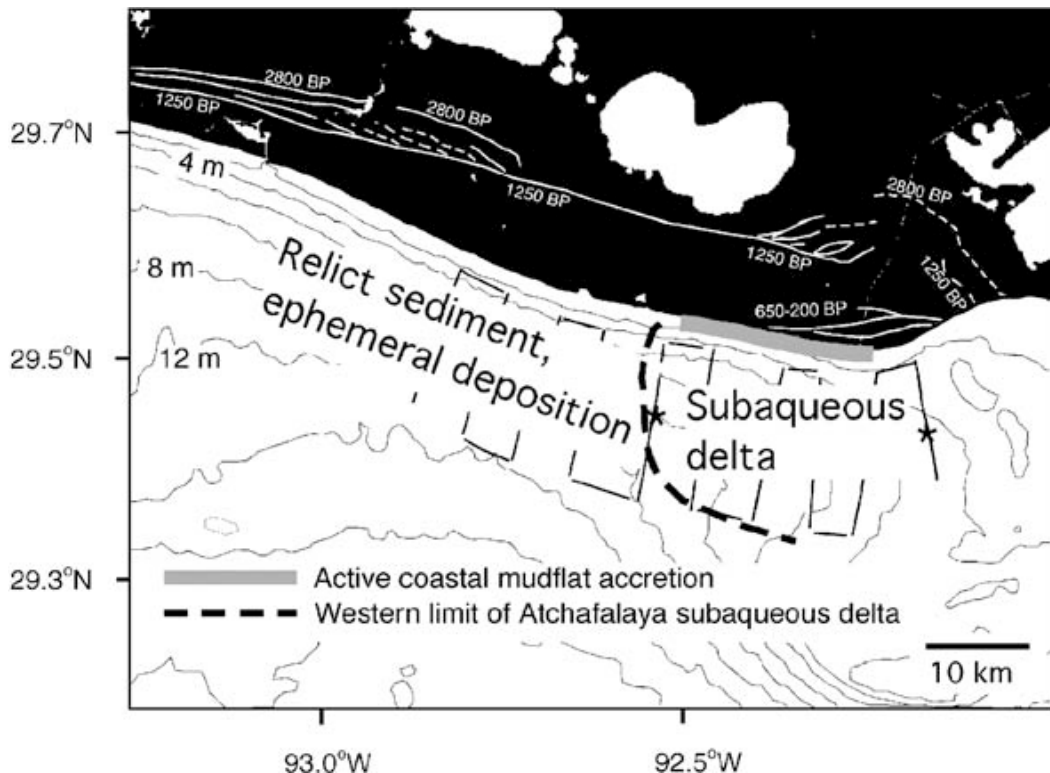

Fig. 5. Western limit of the subaqueous Atchafalaya Delta (dashed line) defined by this study. The shoreline area marked with the gray line indicates an area of active mudflat accretion on the eastern chenier-plain coast. West of this zone, decadal-scale shoreline retreat occurs and coastal mudflats are rare (e.g., Huh et al., 1991; Draut, 2003). East of this accreting zone, minor net shoreline

retreat occurs, though ephemeral mudflats do form there. The prograding mudflat zone corresponds to the area of the eastern chenier-plain inner shelf where this study has found active accumulation (inside the distal-delta boundary). Seaward of the eroding central chenier-plain coast, the inner shelf contains relict sediment and does not currently experience accumulation (outside the delta boundary).

shallow deltaic environment, which can complicate evaluation of the regional sediment budget. How-ever, the fairly consistent composition and gradually decreasing thickness of recent Atchafalaya sediment among the cores where it was detected imply that such a mass can be approximated for the study area considered. A minimum accumulation rate is derived from the ^{210}Pb profile in Core OF. The upper 0.5 m of mud is interpreted to have accumulated within the last 100 years. At 0.5 cm/ yr, this results in a more conservative rate than the 0.94±0.15 cm/yr obtained from the CRS model above, and is considered an appropriate approximate rate to apply to the study area as a whole, given that the accumulation of Atchafalaya sediment gradually decreases to the west of Site OF. Core OF alone is used to estimate this accumula-tion rate because Core OI showed evidence of sediment reworking and a disturbed ^{210}Pb profile. Assuming a constant thickness of 0.5 m over the area spanned by Transects T1–T11, where Atchafalaya sediment has been inferred, and using a bulk density of 1680 kg/m^3 (average bulk density of sediment in the upper 0.5 m of Core OF), the volume of sediment considered is equivalent to 56 x 10^7

metric tons, or 56 x 10^5 metric tons of accumulated sediment per year. Allison et al. (2000) estimated the annual sediment discharge of the Atchafalaya River to be 84 x 10^6 metric tons, based on analysis of four decades of sediment concentration and water discharge data collected by the US Army Corps of Engineers. Of that sediment load, 83% is fine-grained sediment, or ~70 x 10^6 metric tons annually. By this estima-tion, therefore, ~6.3% of the total Atchafalaya sediment load is deposited annually in the inner-shelf area considered (or ~7.6% of the river's fine sediment).

An additional allowance is made for sediment accumulating landward of Transects T1–T11, in the coastal zone where intertidal mudflats are actively accreting. To account for near-shore accumulation, a minimum thickness of 1.0 m of recent sediment is assumed (based on isotopic profiles of 10 near-shore cores studied by Draut, 2003) to deposit between the landward limit of the acoustic transects and the high tide mark onshore. At a density of 1300 kg/m^3, this near-shore accumulation is equivalent to ~0.5% of the Atchafalaya sediment discharge (0.6% of the fine sediment load). The combination of coastal-zone and distal-delta area considered in this study, then, may be a sink for ~7±2% of the total sediment carried by the Atchafalaya River, or ~8±2% of the fine sediment load.

Using a contour plot of ^{210}Pb accumulation rates generated from the cores and acoustic data in this study, combined with 25 cores and Chirp seismic data collected by Allison and Neill (2002) and Neill and Allison (submitted), an

annual accumulation of ~23 x 10^6 metric tons/yr is estimated to occur on the portion of the subaqueous delta outside Atchafalaya Bay where accumulation rates have been shown to exceed 0.5 cm/ yr (Fig. 6; a bulk density of 1680 kg/m^3 is assumed). This figure excludes accumulation that may occur on and seaward of Trinity and Ship Shoals, where Atchafalaya sediment is sparse and unevenly distributed. Accumulation rates shown in Fig. 6 can show spatial and temporal variation; occasional hurricanes and tropical storms also affect the distribution of sand and mud on this continental shelf (e.g., Hurricane Lili in October 2002). That mass is equivalent to ~27% of the annual sediment load of the Atchafalaya River (Allison et al., 2000), which is reasonably consistent with an estimate by Gordon et al. (2001) that 31% of the river's sediment load accumulates annually in their study area south and west of the river mouth.

An additional 27% of the river's sediment is retained in Atchafalaya Bay (23 x 10^6 metric tons/ yr, which at a bulk density of 1680 kg/m^3 corresponds to the sediment volume of 14 x 10^6 m^3 estimated by Wells et al. (1984) to be added to Atchafalaya Bay annually). At present, therefore, estimated accumulation rates in Atchafalaya Bay and on regions of the subaqueous delta that have been studied account for ~54% of the river's annual sediment load. The remaining 46% is assumed to be distributed among the southeastern subaqueous delta (southeast of Point au Fer) where accumulation rates have not been studied in detail, the zone of shoals, where facies distribution is spatially and temporally variable, deeper water where accumulation

occurs at rates < 0.5 cm/yr, and westward transport by longshore currents. Of these possible sinks for the Atchafalaya sediment that remains unaccounted for, a substantial proportion is likely transported to the west by the coastal current (e.g., Wells and Roberts, 1981).

4.2. Relict sediment: central chenier-plain inner shelf

In contrast to the homogeneous mud within the distal Atchafalaya Delta, facies seaward of the central chenier plain (Cores OMLb, OBC, and the lowest 0.3 m of OC) displayed highly variable composition and particle size. Individual stratigraphic horizons are not readily correlated between cores. Radionuclide profiles, vertical facies heterogeneity, and the consolidation of the sediment suggest that the central chenier-plain inner shelf is presently a zone of sediment bypass, where relict material is exposed at the sea floor.
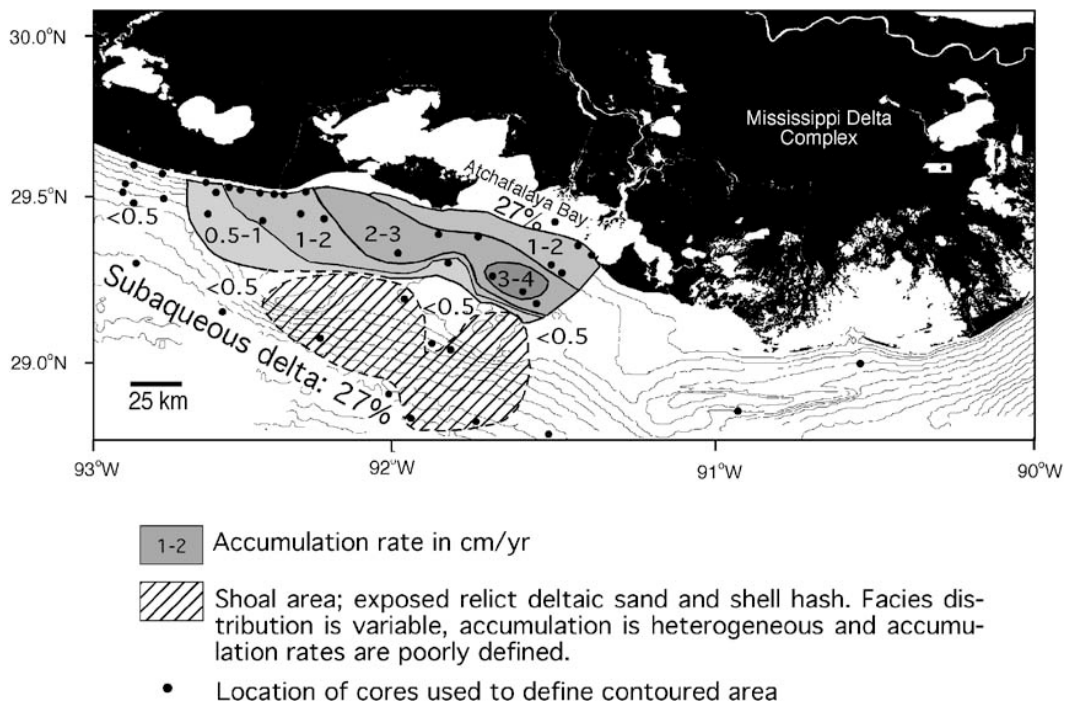
Fig. 6. Contour plot of sediment accumulation on the inner continental shelf seaward and west of Atchafalaya Bay, generated from shallow acoustic data and 25 ^{210}Pb profiles from Neill and Allison (submitted) and Allison and Neill (2002), combined with the five cores and acoustic transects of this study and 10 near-shore push cores collected by Draut (2003). Shaded contoured areas indicate regions of broadly equivalent accumulation rate. Areas where ^{210}Pb profiles indicate accumulation rates of less than 0.5 cm/yr are excluded from this calculation, as are several core sites located far enough east that they may have contained sediment from the main Mississippi outlet. The hatched area indicates shoals where relict sediment is exposed; Atchafalaya sediment accumulation there is heterogeneous and poorly defined. The area inside each contoured region was used to calculate a volume of sediment deposited annually, with no accumulation assumed in the shoal zone. For calculation purposes, the rate inside each contoured area is taken to be the average of accumulation rates on the bounding contours (e.g., a rate of 2.5 cm/yr was assumed for the area marked '2–3 cm/yr' on the map). Sediment volume was converted to mass using a bulk density of 1680 kg/m^3. The total mass deposited in the entire contoured region represents ~27% of the annual sediment load of the Atchafalaya River. Significant variability in the rates and locations of sedimentation may alter the accumulation patterns shown in this contoured region over time; hurricane and tropical storm activity (e.g., Hurricane Lili in 2002) can also affect the distribution of sediment on this continental shelf. Sediment accumulating in Atchafalaya

Bay has been estimated to account for an additional ~27% of the annual Atchafalaya sediment load (Wells et al., 1984).

4.2.1. Age and source of relict sediment

Radiocarbon analyses of shell material yielded reservoir-corrected ages of 1263–1463±60 years BP in Core OBC (at 0.51 m bsf) and 1113–131±30 years BP in Core OMLb (at 0.41 m bsf). These ages reflect the average time at which the shells ceased to grow. While not conclusively defining the age of deposition, these ages define a maximum deposition age for sediment above the shell horizons. Constraining a minimum deposi- tion age for sediment above the dated shell horizons is more difficult. The lack of excess ^{210}Pb (Figs. 3d and e) implies that deposition occurred more than 100 years ago; the greater consolidation of clay in these cores compared to the 250-year-old basal Atchafalaya mud in Core OF suggests that the relict clay and silt in Core OMLb is considerably older (perhaps by as much as several centuries) than 250 yr BP. Sediment below the dated shell layers is of uncertain age.

The most probable source for relict siliciclastic sediment on the central chenier plain was the Lafourche lobe, at the western edge of the Mississippi Delta complex (Fig. 1), the activity of which immediately preceded development of the modern (Balize) course. Reported dates of activity vary but the most recent assessment (Törnqvist et al., 1996) places its first activation at ~1500 BP (Table 1). The ^{14}C-based shoreline chronology of Gould and McFarlan (1959)

supports chenier plain accretion during activity of the Lafourche Delta lobe. Progradation on the chenier plain is tied to activity on the Teche, Lafourche, and nascent Atchafalaya Delta lobes, and erosion (chenier-ridge development and formation of relict shorelines) to activity on the St. Bernard and modern (Balize–Plaquemines) lobes (Fig. 1). The last major progradation on the chenier plain, before delivery of Atchafalaya sediment, corre-sponds to Lafourche lobe activity from 1200 to 600 BP (Fig. 2b; Gould and McFarlan, 1959). Simultaneous accumulation on the chenier-plain inner shelf due to Lafourche lobe activity (1200–600 BP), as suggested by Cores OBC and OMLb, appears probable.

4.2.2. Development of stratal geometry

On multiple spatial scales, the stratigraphy in relict sediment of the central chenier-plain shelf differs from that of the eastern chenier plain, where Atchafalaya sediment dominates. Acoustic transects show seaward-dipping reflectors truncated by the sea floor (Transects T15–T19; Fig. 4e and f), in contrast to the actively accreting topset–foreset–bottomset clinoform stratigraphy of the eastern chenier plain. Cores OBC and OMLb contained layers of sand and shell hash that corresponded to the depths at which acoustic reflectors occur. These relationships strongly suggests sigmoidal clinoforms that have been ablated and cut by an erosion surface that dips seaward more steeply than the bedding angle. These reflectors are interpreted as remnants of clinoform stratigraphy that formed during accumulation of Lafourche lobe sediment. Their modern geometry is interpreted to reflect the transition from chenier-plain accretion to erosion

that accompanied the shift from Lafourche to modern (Balize) sedimentation on the Mississippi Delta plain. Rapid accumulation on the central chenier-plain shelf during the Lafourche phase of accretion is proposed to have generated clinoforms similar to those on the prograding Atchafalaya Delta. The transition from accreting to eroding conditions resulted in clinoform ablation and the development of a hiatal sea floor surface on which no long-term accumulation now occurs.

Vertical facies heterogeneity in relict chenierplain sediment may be related to post-storm deposition; sand–mud couplets can result from decreasing energy during a waning storm. Coarse horizons overlain by finer units in Cores OBC and OMLb form a vertical sequence similar to facies interpreted as storm beds (Reineck and Singh, 1972; Morton and Winker, 1979; Morton, 1988; Bentley and Nittrouer, 1999). Alternatively, coarse shell horizons may reflect reduced supply of fine-grained sediment. Shell material occurs in fine-grained horizons in relict and modern sediment on the Louisiana shelf. During periods of reduced sediment delivery to the chenier-plain area, hor-izons of concentrated shell material may form that later become overlain by mud when fine-grained delivery is resumed. For the millimeter-scale silt/ clay laminations within fine-grained horizons of Core OMLb, a storm origin is possible but is not required. These beds may have been deposited during fluvial pulses that brought episodically high sediment load to the chenier-plain area. Similar laminations are visible today on the proximal subaqueous Atchafalaya Delta immediately seaward of Atchafalaya

Bay (Allison and Neill, 2002), where fluvial flood layers are deposited.

4.3. Future development of the chenier plain

Previous studies have indicated that the eastern chenier plain is prograding at rates of tens of meters per year, while other sections of this coast are retreating (e.g., Morgan and Larimore, 1957; Adams et al., 1978; Wells and Kemp, 1981; Draut, 2003). Presently, the eastern chenier plain is undergoing net accretion in response to growth of the subaqueous Atchafalaya Delta. The area where sediment is accumulating on the inner shelf (Transects T1–T7) corresponds to the section of the coast where mudflat progradation occurs due to shoreward sediment transport during cold front events (Fig. 5). The central chenier-plain coast, where relict sediment is exposed on the inner shelf, is currently undergoing decadal-scale shoreline retreat in a similar manner to most areas of the Louisiana coast (e.g., Draut, 2003). The lack of modern coastal accretion on the central chenier plain is consistent with the lack of long-term accumulation on the adjacent inner shelf. As deltaic sediment migrates to the west, the central chenier plain may eventually experience similar accretion as the influence of Atchafalaya sedimentation extends farther west along the inner shelf. As this occurs, the erosion surface that forms the sea floor on the central chenier-plain shelf will become the base of a new Atchafalaya sedimentary sequence. Sedimentation rates on the chenier plain, and on the Atchafalaya Delta in general, will likely increase after Atchafalaya Bay is filled (Tye and Coleman, 1989); the filling of this bay at the river's mouth will lead to sediment bypass of the present Atchafalaya Bay depocenter and

increased deposition seaward of the Point au Fer reef (Fig. 2a). Bypassing of Atchafalaya Bay will increase the amount of sediment available for westward transport to the chenier plain. It has been estimated that Atchafalaya Bay will be filled within the next 40 years (Wells et al., 1984). This scenario is proposed for the development of the chenier plain if the Atchafalaya distributary were to develop naturally. The growth of the Atchafalaya distributary is limited by the control structure designed to prevent capture of the main Mississippi course, and by reduced sediment load in the Mississippi River system due to human activity in the drainage basin (Keown et al., 1986; Kesel, 1988). For these reasons, the Atchafalaya Delta system is not expected to develop the vast spatial extent and widespread stratigraphic influence that the Lafourche lobe had during its activity, at least in the near future.

5. Conclusions

Sedimentary, geochemical, and acoustic studies of this mud-dominated coastal system show that the influence of the Atchafalaya River on inner-shelf sedimentation is ephemeral west of ~92.55°W. East of that delta boundary, Atchafa-laya mud accumulates as the sigmoidal clinoform progrades. These distal deposits on the eastern chenier-plain shelf are well mixed by biogenic and physical processes. Coastal mudflat accretion on the eastern chenier plain corresponds to the location on the inner shelf where underconsolidated Atchafalaya sediment is present. Mass-balance calculations indicate that the eastern chenier-plain coast and inner shelf may be a sink for ~7±2% of the total fluvial sediment load. Approximately 57% of the Atchafalaya sediment load can be accounted for with

current estimates of accumulation rates in Atchafalaya Bay and on the distal subaqueous delta. West of ~92.55°W, on the central chenier-plain shelf, relict sediment is exposed on the sea floor that was originally deposited between ~1200 and 600 years BP, during activity of the Lafourche lobe of the Mississippi Delta complex, when major coastal progradation occurred on the chenier plain. The coast and inner shelf of the central chenier plain currently experience erosion, a trend which may reverse in the future as the influence of Atchafalaya sedimentation extends farther west.

References

Adams, R.D., Banas, P.J., Baumann, R.H., Blackman, J.H., McIntire, B.W.G., 1978. Shoreline erosion in coastal Louisiana: inventory and assessment. Final report to Louisiana Department of Transportation and Development (139pp).

Alexander, C.A., DeMaster, D.J., Nittrouer, C.A., 1991. Sediment accumulation in a modern epicontinental-shelf setting: the Yellow Sea. Marine Geology 98, 51–72.

Allison, M.A., Neill, C.F., 2002. Accumulation rates and stratigraphic character of the modern Atchafalaya River prodelta, Louisiana. Transactions—Gulf Coast Association of Geological Societies 52, 1031–1040.

Allison, M.A., Nittrouer, C.A., Faria Jr., L.E.C., 1995a. Rates and mechanisms of shoreface progradation and retreat downdrift of the Amazon river mouth. Marine Geology 125, 373–392.

Allison, M.A., Nittrouer, C.A., Kineke, G.C., 1995b. Seasonal sediment storage on mudflats adjacent to the Amazon River. Marine Geology 125, 303–328.

Allison, M.A., Kuehl, S.A., Martin, T.C., Hassan, A., 1998. Importance of flood–plain sedimentation for river sediment budgets and terrigenous input to the oceans: insights from the Brahmaputra–Jamuna River. Geology 26, 175–178.

Allison, M.A., Kineke, G.C., Gordon, E.S., Goñi, M.A., 2000. Development and reworking of a seasonal flood deposit on the inner continental shelf off the Atchafalaya River. Continental Shelf Research 20, 2267–2294.

Appleby, P.G., Oldfield, F., 1978. The calculation of lead-210 dates assuming a constant rate of supply of unsupported ^{210}Pb to the sediment. Catena 5, 1–8.

Augustinius, P.G.E.F., 1989. Cheniers and chenier plains: a general introduction. Marine Geology 90, 219–229.

Baskaran, M., Santschi, P.H., 2002. Particulate and dissolved ^{210}Pb activities in the shelf and slope regions of the Gulf of Mexico waters. Continental Shelf Research 22, 1493–1510.

Beall Jr., A.O., 1968. Sedimentary processes operative along the western Louisiana shoreline. Journal of Sedimentary Petrology 38, 869–877.

Bentley, S.J., Nittrouer, C.A., 1999. Physical and biological influences on the formation of sedimentary fabric in an oxygen-restricted depositional environment: eckenförde Bay, southwestern Baltic Sea. Palaios 14, 585–600.

Brannon Jr., H.R., Simons, L.H., Perry, D., Daughtry, A.C., McFarlan Jr., E., 1957. Humble oil company radiocarbon dates II. Science 125, 919–923.

Byrne, J.V., LeRoy, D.O., Riley, C.M., 1959. The chenier plain and its stratigraphy, southwestern Louisiana. Transactions—Gulf Coast Association of Geological Societies 9, 237–260.

Coakley, J.P., Syvitski, J.P.M., 1991. SediGraph technique. In: Syvitski, J.P.M. (Ed.), Principles, Methods, and Application of Particle Size Analysis. Cambridge University Press, Cambridge (368pp).

Coleman, J.M., 1981. Deltas: Processes of Deposition and Models for Exploration. Burgess Publishing Company, Minneapolis, MN (124pp).

Coleman, J.M., 1988. Dynamic changes and processes in the Mississippi River delta. Geological Society of America Bulletin 100, 999–1015.

Coleman, J.M., Gagliano, S.M., 1964. Cyclic sedimentation in the Mississippi River deltaic plain. Transactions—Gulf Coast Association of Geological Societies 14, 67–80.

Coleman, J.M., Gagliano, S.M., 1965. Sedimentary structures: Mississippi River deltaic plain. In: Middleton, G.V. (Ed.), Primary Sedimentary Structures and Their Hydrodynamic Interpretation, vol. 12. SEPM Special Publication, pp, pp. 133–148.

Crozaz, G., Picciotto, E., De Breuck, W., 1964. Antarctic snow chronology with ^{210}Pb. Journal of Geophysical Research 69, 2597–2604.

Draut, A.E., 2003. Fine-grained sedimentation on the chenier plain coast and inner continental shelf, northern Gulf of Mexico. Ph.D. Thesis 2003–08, Massachusetts Institute of Technology–Woods Hole Oceanographic Institution, Cambridge, MA (369pp).

Draut, A.E., Kineke, G.C., Huh, O.K., Grymes, J.M., Westphal, K.A., Moeller, C.C., submitted. Coastal mudflat accretion under energetic conditions. Marine Geology, in review.

Duursma, E.K., Gross, M.G., 1971. Marine sediments and radioactivity. In: Radioactivity in the Marine Environment. Panel on Radioactivity in the Marine Environment of the Committee on Oceanography, National Research Council. National Academy of Sciences, Washington, DC, pp. 147–160.

Fairbanks, R.G., 1989. A 17,000-year glacio-eustatic sea level record: influence of glacial melting rates on the Younger Dryas event and deep-ocean circulation. Nature 342, 637–642.

Fisk, H.N., 1944. Geological investigation of the alluvial valley of the lower Mississippi River. US Army Corps of Engineers, Mississippi River Commission, Vicksburg, MS.

Fisk, H.N., McFarlan Jr., E., 1955. Late Quaternary deltaic deposits of the Mississippi River—local sedimentation and basin tectonics. In: Poldervaart, A. (Ed.), Crust of the Earth, a Symposium. Geological Society of America Special Paper 62, 279–302.

Frazier, D.E., 1967. Recent deposits of the Mississippi River, their development and chronology. Transactions—Gulf Coast Association of Geological Societies 17, 287–315.

Gaöggler, H., Von Gunten, H.R., Nyffeler, V., 1976. Determination of ^{210}Pb in lake sediments and air samples by direct gamma-ray measurement. Earth and Planetary Science Letters 33, 119–121.

Gagliano, S.M., Meyer-Arndt, K.J., Wicker, K.M., 1981. Land loss in the Mississippi River deltaic plain. Transactions—Gulf Coast Association of Geological Societies 31, 295–300.

Gon˜ i, M.A., Ruttenburg, K.C., Eglinton, T.I., 1998. A reassessment of the sources and importance of land-derived organic matter in surface sediments from the Gulf of Mexico. Geochimica et Cosmochimica Acta 62, 3055–3075.

Goodbred Jr., S.L., Kuehl, S.A., 1998. Floodplain processes in the Bengal Basin and storage of Ganges–Brahmaputra river sediment: an accretion study using ^{137}Cs and Pb geochronology. Sedimentary Geology 121, 239–258. Gordon, E.S., Gon˜ i, M.A., Roberts, Q.N.,

Kineke, G.C., Allison, M.A., 2001. Organic matter distribution and accumulation on the inner Louisiana shelf west of the Atchafalaya River. Continental Shelf Research 21, 1691–1721.

Gould, H.R., McFarlan Jr., E., 1959. Geologic history of the chenier plain, southwestern Louisiana. Transactions—Gulf Coast Association of Geological Societies 9, 261–274.

Harris, P.T., Baker, E.K., Cole, A.R., Short, S.A., 1993. A preliminary study of sedimentation in the tidally dominated Fly River delta, Gulf of Papua. Continental Shelf Research 13, 441–472.

Holmes, C.W., 1985. Natural radioisotope ^{210}Pb as an indicator of origin of fine-grained sediment. Geo-Marine Letters 4, 203–206.

Hoyt, J.H., 1969. Chenier versus barrier genetic and stratigraphic distinction. American Association of Petroleum Geologists Bulletin 53, 299–306.

Huh, O.K., Roberts, H.H., Rouse, L.J., Rickman, D.A., 1991. Fine grain sediment transport and deposition in the Atchafalaya and chenier plain sedimentary system. Coastal Sediments '91, 817–830.

Huh, O.K., Walker, N.D., Moeller, C., 2001. Sedimentation along the eastern chenier plain coast: down drift impact of a delta complex shift. Journal of Coastal Research 17, 72–81.

Jaeger, J.M., Nittrouer, C.A., 1995. Tidal controls on the formation of fine-scale sedimentary strata near the Amazon mouth. Marine Geology 125, 259–281.

Joshi, S.R., 1987. Nondestructive determination of lead-210 and radium-226 in sediments by direct photon analysis.

Journal of Radioanalytical and Nuclear Chemistry 116, 169–212.

Kemp, G.P., 1986. Mud deposition at the shoreface: wave and sediment dynamics on the chenier plain of Louisiana. Ph.D. Thesis, Louisiana State University, Baton Rouge, LA (146pp).

Keown, M.P., Dardeau Jr., E.A., Causey, E.M., 1986. Historic trends in the sediment flow regime of the Mississippi River. Water Resources Research 22, 1555–1564.

Kesel, R.H., 1988. The decline in the suspended load of the lower Mississippi River and its influence on adjacent wetlands. Environmental Geology and Water Science 11, 271–281.

Kineke, G.C., 2001a. The role of fluid mud in sediment transport processes along a muddy coast. Report to the Office of Naval Research, Grant N00014-98-0083, Fiscal Year 2001: http://www.onr.navy.mil/sci_tech/ocean/ reports/docs/cd/01/cdkine01.pdf.

Kineke, G.C., 2001b. Fine-sediment dispersal and accumulation on the shallow Louisiana shelf. Eos, Transactions of the American Geophysical Union 82(47), Fall Meeting Supplement, Abstract OS22B-03.

Kineke, G.C., Hart, K.A., Velasco, D.W., Allison, M.A., 2001. The role of short time-scale resuspension events in dispersal of Atchafalaya River sediment on the shallow shelf, Gulf of Mexico (Poster). American Geophysical Union Chapman Conference on the Formation of Strata on Continental Margins, Ponce, PR.

Knudsen Engineering, Ltd., 1996. Knudsen 320B Series Black-box Echosounder Operator's Manual. Knudsen Engineer-ing, Ltd., Perth, Ont.

Kolb, C.R., Van Lopik, J.R., 1958. Geology of the Mississippi River deltaic plain, southeastern Louisiana. US Army Corps of Engineers Waterways Experiment Station, Vicks-burg, MS, Technical Report 3-483.

Kuehl, S.A., Nittrouer, C.A., DeMaster, D.J., Curtin, T.B., 1985. A long, square-barrel gravity corer for sedimentolo-gical and geochemical investigation of fine-grained sedi-ments. Marine Geology 62, 365–370.

Kuehl, S.A., Hariu, T.M., Moore, W.S., 1990. Shelf sedimentation off the Ganges–Brahmaputra river system: evidence for sediment bypassing to the Bengal Fan. Geology 17, 1132–1135.

Kuehl, S.A., Pacioni, T.D., Rine, J.M., 1995. Seabed dynamics of the inner Amazon continental shelf: temporal and spatial variability of surficial strata. Marine Geology 125, 283–302.

Lee, H.J., Chough, S.K., 1987. Technical note—bulk density, void ratio, and porosity determined from average grain density and water content: an evaluation of errors. Marine Geotechnology 7, 53–62.

Levin, D.R., 1991. Transgressions and regressions in the Barataria bight region of coastal Louisiana. Transac-tions—Gulf Coast Association of Geological Societies 41, 408–431.

Livingston, H.D., Bowen, V.T., 1979. Pu and ^{137}Cs in coastal sediments. Earth and Planetary Science Letters 43, 29–45.

McCave, I.N., Syvitski, J.P.M., 1991. Principles and methods of geological particle size analysis. In: Syvitski, J.P.M. (Ed.), Principles, Methods, and Application of Particle Size Analysis. Cambridge University Press, Cambridge (368pp).

McFarlan Jr., E., 1961. Radiocarbon dating of late Quaternary deposits, south Louisiana. Geological Society of America Bulletin 72, 129–158.

Micromeritics Inc., 2001. SediGraph 5100 Operator's Manual. Micromeretics Inc., Norcross, GA.

Miller, K.M., Heit, M., 1986. A time resolution methodology for assessing the quality of lake sediment cores that are dated by ^{137}Cs. Limnology and Oceanography 31, 1292–1300.

Milliman, J.D., Meade, R.H., 1983. World-wide delivery of river sediment to the ocean. Journal of Geology 91, 1–21.

Morgan, J.P., Larimore, P.B., 1957. Changes in the Louisiana shoreline. Transactions—Gulf Coast Association of Geological Societies 7, 303–310.

Morgan, J.P., Van Lopik, J.R., Nichols, L.G., 1953. Occurrence and development of mudflats along the western Louisiana coast. Technical Report No. 2, Coastal Studies Institute, Louisiana State University, Baton Rouge, LA (34pp).

Morgan, J.P., Nichols, L.G., Wright, M., 1958. Morphologic effects of Hurricane Audrey. Technical Report 10, Coastal Studies Institute, Louisiana State University, Baton Rouge, LA. Morton, R.A., 1981. Formation of storm deposits by wind-forced currents in the Gulf of Mexico and the North Sea. International

Association of Sedimentologists Special Publication 5, 385–396.

Morton, R.A., 1988. Nearshore response to great storms. In: Clifton, H.E. (Ed.), Sedimentologic Consequences of Convulsive Geologic Events. Geological Society of America Special Paper 229, 7–22.

Morton, R.A., Winker, C.D., 1979. Distribution and significance of coarse biogenic and clastic deposits on the Texas inner shelf. Transactions—Gulf Coast Association of Geological Societies 29, 306–320.

Neill, C.F., Allison, M.A., submitted. Subaqueous delta formation on the Atchafalaya shelf, Louisiana. Marine Geology, in review.

Nemec, W., 1995. The dynamics of deltaic suspension plumes. In: Oti, M.N., Postma, G. (Eds.), Geology of Deltas. A.A. Balkema, Rotterdam, The Netherlands, pp. 31–93.

Nittrouer, C.A., Sternberg, R.W., Carpenter, R., Bennett, J.T., 1979. The use of Pb-210 geochronology as a sedimentary tool: application to the Washington continental shelf. Marine Geology 31, 297–316.

Nittrouer, C.A., Kuehl, S.A., DeMaster, D.J., Kowsmann, R.O., 1986. The deltaic nature of Amazon shelf sedimentation. Geological Society of America Bulletin 97, 444–458.

Nittrouer, C.A., Kuehl, S.A., Sternberg, R.W., Figueiredo Jr., A.G., Faria, L.E.C., 1995. An introduction to the geological significance of sediment transport and accumulation on the Amazon continental shelf. Marine Geology 125, 177–192.

Otvos, E.G., Price, W.A., 1979. Problems of chenier genesis and terminology—an overview. Marine Geology 31, 252–263.

Penland, S., Ramsey, K.E., 1990. Relative sea-level rise in Louisiana and the Gulf of Mexico: 1908–1988. Journal of Coastal Research 6, 323–342.

Penland, S., Suter, J.R., 1989. The geomorphology of the Mississippi River chenier Plain. Marine Geology 90, 231–258.

Penland, S., Suter, J.R., McBride, R.A., 1987. Delta plain development and sea level history in the Terrebonne coastal region, Louisiana. Coastal Sediments '87, 1689–1705.

Penland, S., Suter, J.R., Sallenger Jr., A.H., Williams, S.J., McBride, R.A., Westphal, K.E., Reimer, P.D., Jaffe, B.E., 1989. Morphodynamic signature of the 1985 hurricane impacts on the northern Gulf of Mexico. Coastal Zone '89, Proceedings of the Sixth Symposium on Coastal and Ocean Management 6, 4220–4234.

Penland, S., Roberts, H.H., Williams, S.J., Sallenger Jr., A.H., Cahoon, D.R., Davis, D.W., Groat, C.G., 1990. Coastal land loss in Louisiana. Transactions—Gulf Coast Association of Geological Societies 40, 685–699.

Penland, S., Wayne, L., Britsch, L.D., Williams, S.J., Beall, A.D., Butterworth, V.C., 2000. Process classification of coastal land loss between 1932 and 1990 in the Mississippi River delta plain, southeastern Louisiana. US Geological Survey Open File Report, OFR-00-418, Reston, VA.

Postma, G., 1990. In: Colella, A., Prior, D.B. (Eds.), Deposi-tional Architecture and Facies of River and Fan Deltas: a Synthesis. International Association of Sedimentologists

Special Publication 10, 13–27.

Postma, G., 1995. Causes of architectural variation in deltas. In: Oti, M.N., Postma, G. (Eds.), Geology of Deltas. A.A. Balkema, Rotterdam, The Netherlands, pp. 3–16.

Reineck, H.E., Singh, I.B., 1972. Genesis of laminated sand and graded rhythmites in storm-sand layers of shelf mud. Sedimentology 18, 123–128.

Roberts, H.H., 1997. Dynamic changes of the Holocene Mississippi River delta plain: the delta cycle. Journal of Coastal Research 13, 605–627.

Roberts, H.H., Adams, R.D., Cunningham, R.H., 1980. Evolution of sand-dominant subaerial phase, Atchafalaya Delta, Louisiana. American Association of Petroleum Geologists Bulletin 64, 264–279.

Roberts, H.H., Huh, O.K., Hsu, S.A., Rouse Jr., L.J., Rickman, D.A., 1987. Impact of cold-front passages on geomorphic evolution and sediment dynamics of the complex Louisiana coast. Coastal Sediments 87, 1950–1963.

Roberts, H.H., Huh, O.K., Hsu, S.A., Rouse Jr., L.J., Rickman, D.A., 1989. Winter storm impacts on the chenier plain coast of southwestern Louisiana. Transactions—Gulf Coast Association of Geological Societies 39, 515–522.

Roberts, H.H., Walker, N., Cunningham, R., Kemp, G.P., Majersky, S., 1997. Evolution of sedimentary architecture and surface morphology: Atchafalaya and Wax Lake deltas, Louisiana (1973–1994). Transactions—Gulf Coast Association of Geological Societies 47, 477–484.

Roberts, H.H., Bentley, S., Coleman, J.M., Hsu, S.A., Huh, O.K., Rotondo, K., Inoue, M., Rouse Jr., L.J., Sheremet, A., Stone, G., Walker, N., Welsh, S., Wiseman Jr., W.J.,

2002. Geological framework and sedimentology of recent mud deposition on the eastern chenier plain coast and adjacent inner shelf, western Louisiana. Transactions—Gulf Coast Association of Geological Societies 52, 849–859.

Rotondo, K.A., Bentley, S.J., 2002. Fluid mud sedimentation on the innermost western Louisiana shelf. Eos, Transactions of the American Geophysical Union 83(4), Ocean Science Meeting Supplement, Abstract OS11G-890.

Rotondo, K.A., Bentley, S.J., 2003. Deposition and resuspension of fluid mud on the western Louisiana inner shelf. Transactions—Gulf Coast Association of Geological Societies 53, 722–731.

Rouse Jr., L.J., Roberts, H.H., Cunningham, R.H.W., 1978. Satellite observation of the subaerial growth of the Atchafalaya Delta, Louisiana. Geology 6, 405–408.

Russell, R.J., Howe, H.V., 1935. Cheniers of southwestern Louisiana. Geographical Review 25, 449–461.

Saucier, R.T., 1963. Recent geomorphic history of the Ponchartrain Basin. Louisiana State University, Coastal Studies Series 9 (114pp).

Saucier, R.T., 1994. Geomorphology and Quaternary Geologic History of the Lower Mississippi Valley. Mississippi River Commission, Vicksburg, MS (364pp).

Schlemon, R.J., 1975. Subaqueous delta formation—Atchafa-laya Bay, Louisiana. In: Broussard, M.L. (Ed.), Deltas. Houston Geological Society, Houston, TX, pp. 209–221. Scrudato, R.J., Estes, E.L., 1976. Clay–lead sorption relations. Environmental Geology 1, 167–170.

Scruton, P.C., 1960. Delta building and the deltaic sequence. In: Shepard, F.P., Phleger, F.B., Van Andel, T.H. (Eds.), Recent Sediments, Northwest Gulf of Mexico. American Association of Petroleum Geologists, Tulsa, OK, pp. 82–102.

or Sholkovitz, E.R., Mann, D.R., 1984. The pore water chemistry 239, 240$_{Pu}$ and ^{137}Cs in sediments of Buzzards Bay, Massachusetts. Geochimica et Cosmochimica Acta 48, 1107–1114.

Sholkovitz, E.R., Cochran, J.K., Carey, A.E., 1983. Laboratory studies of the diagenesis and mobility of ^{239,240}Pu and ^{137}Cs in nearshore sediments. Geochimica et Cosmochimica Acta 47, 1369–1379.

Smith, J.N., Ellis, K.M., 1982. Transport mechanism for Pb-210, Cs-137 and Pu fallout radionuclides through fluvial-marine systems. Geochimı´ca et Cosmochimica Acta 46, 941–954.

Smith, J.N., Walton, A., 1980. Sediment accumulation rates and geochronologies measured in the Sanguenay fjord using Pb-210 dating method. Geochimica et Cosmochimica Acta 44, 225–240.

Stuiver, M., Pearson, G.W., Braziunas, T., 1986. Radiocarbon age calibration of marine samples back to 9000 cal yr BP. Radiocarbon 28, 980–1021.

Thompson, W.C., 1951. Oceanographic Analysis of Atchafalaya Bay, Louisiana and Adjacent Continental Shelf Areas Marine Pipeline Problems, vol. 2, no. 25. Texas A&M Research Foundation, Department of Oceanography (31pp).

Törnqvist, T.E., Kidder, T.R., Autin, W.J., van der Borg, K., de Jong, A.F.M., Klerks, C.J.W., Snijders, E.M.A., Storms, J.E.P., van Dam, R.L., Wiemann, M.C., 1996. A revised chronology for Mississippi River subdeltas. Science 273, 1693–1696.

Trowbridge, A.C., 1930. Building of Mississippi Delta. American Association of Petroleum Geologists Bulletin 14, 867–901.

Tye, R.S., Coleman, J.M., 1989. Evolution of Atchafalaya lacustrine deltas, south-central Louisiana. Sedimentary Geology 65, 95–112.

Van Heerden, I.L., Roberts, H.H., 1980. The Atchafalaya Delta—Louisiana's new prograding coast. Transactions—Gulf Coast Association of Geological Societies 30, 497–506.

Van Heerden, I.L., Roberts, H.H., 1988. Facies development of the Atchafalaya Delta, Louisiana: a modern bayhead delta. American Association of Petroleum Geologists Bulletin 72, 439–453.

Velasco, D.W., 2003. Shallow stratigraphy observations using electrical resistivity and dual-frequency echo sounding methods. M.S. Thesis, Boston College, Chestnut Hill, MA.

Wells, J.T., Kemp, G.P., 1981. Atchafalaya mud stream and recent mudflat progradation: Louisiana chenier plain. Transactions—Gulf Coast Association of Geological Societies 31, 39–46.

Wells, J.T., Roberts, H.H., 1981. Fluid mud dynamics and shoreline stabilization: Louisiana chenier plain. Proceedings of the Coastal Engineering Conference 17, 1382–1401.

Wells, J.T., Chinburg, S.J., Coleman, J.M., 1984. The Atchafalaya River delta, Report 4: Generic analysis of delta development. US Army Corps of Engineers, Technical Report HL 82–15, Vicksburg, MS.

Westphal, K.A., Matteson, W.H., McBride, R.A., 1991. Historical shoreline change in the northern Gulf of Mexico. Louisiana Geological Survey: Coastal Erosion Subcommittee of the US Environmental Protection Agency, Gulf of Mexico Program.

Williams, S.J. (Ed.), 1994. Processes of Coastal Wetlands Loss in Louisiana. US Geological Survey Open File Report, OFR-94-0275, Reston, VA.

Zangger, E., McCave, I.N., 1990. A redesigned kasten core barrel and sampling technique. Marine Geology 94, 165–171.